Synergistic Roles of Bone Morphogenetic Protein 15 and Growth Differentiation Factor 9 in Ovarian Function

Changning Yan, Pei Wang, Janet DeMayo, Francesco J. DeMayo, Julia A. Elvin, Cecilia Carino, Sarvamangala V. Prasad, Sheri S. Skinner, Bonnie S. Dunbar, Jennifer L. Dube, Anthony J. Celeste, and Martin M. Matzuk

Departments of Pathology (C.Y., M.M.M.), Molecular and Cellular Biology (P.W., J.D., F.J.D., C.C., S.V.P., S.S.S., B.S.D., M.M.M.), and Molecular and Human Genetics (J.A.E., M.M.M.)
Baylor College of Medicine
Houston, Texas, 77030

Department of Tissue Growth and Repair (J.L.D., A.J.C.)
Genetics Institute, Inc.
Cambridge, Massachusetts 02140

Knockout mouse technology has been used over the last decade to define the essential roles of ovarian-expressed genes and uncover genetic interactions. In particular, we have used this technology to study the function of multiple members of the transforming growth factor-β superfamily including inhibins, activins, and growth differentiation factor 9 (GDF-9 or *Gdf9*). Knockout mice lacking GDF-9 are infertile due to a block in folliculogenesis at the primary follicle stage. In addition, recombinant GDF-9 regulates multiple cumulus granulosa cell functions in the periovulatory period including hyaluronic acid synthesis and cumulus expansion. We have also cloned an oocyte-specific homolog of GDF-9 from mice and humans, which is termed bone morphogenetic protein 15 (BMP-15 or *Bmp15*). To define the function of BMP-15 in mice, we generated embryonic stem cells and knockout mice, which have a null mutation in this X-linked gene. Male chimeric and *Bmp15* null mice are normal and fertile. In contrast to *Bmp15* null males and *Gdf9* knockout females, *Bmp15* null females (*Bmp15*$^{-/-}$) are subfertile and usually have minimal ovarian histopathological defects, but demonstrate decreased ovulation and fertilization rates. To further decipher possible direct or indirect genetic interactions between GDF-9 and BMP-15, we have generated double mutant mice lacking one or both alleles of these related homologs. Double homozygote females (*Bmp15*$^{-/-}$*Gdf9*$^{-/-}$) display oocyte loss and cysts and resemble *Gdf9*$^{-/-}$ mutants. In contrast, *Bmp15*$^{-/-}$*Gdf9*$^{+/-}$ female mice have more severe fertility defects than *Bmp15*$^{-/-}$ females, which appear to be due to abnormalities in ovarian folliculogenesis, cumulus cell physiology, and fertilization. Thus, the dosage of intact *Bmp15* and *Gdf9* alleles directly influences the destiny of the oocyte during folliculogenesis and in the periovulatory period. These studies have important implications for human fertility control and the maintenance of fertility and normal ovarian physiology. (Molecular Endocrinology 15: 854–866, 2001)

0888-8809/01/$3.00/0
Molecular Endocrinology 15(6): 854–866

INTRODUCTION

Although important molecular events occur during all stages of mammalian ovarian folliculogenesis, few oocyte-expressed regulatory proteins have been identified. Our group and others have used embryonic stem (ES) cell technology to produce mouse models with ovarian abnormalities (for review, see Refs. 1 and 2). These knockout mouse models demonstrate defects in germ cell maintenance, proliferation, and development [*e.g.* Dazla knockout mice (3)], formation of primordial follicles [*e.g.* Figα knockout mice (4)], formation of secondary follicles [*e.g. Gdf9* knockout mice (5)], formation of antral follicles [*e.g.* FSHβ knockout mice (6)], ovulation [*e.g.* cyclooxygenase 2 (7) and progesterone receptor knockout mice (8)], or postovulation [*e.g.* Mater knockout mice (9)]. Whereas mutations in oocyte-expressed genes (*e.g.* Figα, kit receptor, and Mater) result in intrinsic defects in the oocyte or early embryo (4, 9, 10), growth differentiation factor 9 (GDF-9) is the only known oocyte-secreted growth factor that is required for somatic cell

function in mice *in vivo*. Using *Gdf9* knockout mice, we have shown that GDF-9 is directly required for granulosa cell growth and differentiation and indirectly for oocyte meiotic competence and formation of a theca (5, 11, 12).

Gdf9 mRNA and GDF-9 protein are not only expressed at the primary follicle stage but are also present in oocytes through ovulation (13–15). Since mice lacking GDF-9 have a block at the primary follicle stage, fail to form a theca, and eventually demonstrate defects in meiotic competence, it was unclear from these knockout studies whether GDF-9 also plays a role at later stages of folliculogenesis. It was therefore important to determine the function of GDF-9 in the periovulatory period since oocyte-secreted growth factors had been identified to play key regulatory functions in this period. Using recombinant mouse GDF-9, we demonstrated that GDF-9 can regulate a diverse number of genes and processes in the periovulatory stage, including cumulus expansion, induction of hyaluronan synthase 2, cyclooxygenase 2, and the EP2 PGE_2 receptor, and inhibition of LH receptor and urokinase plasminogen activator (13, 15, 16). In addition, recombinant rat GDF-9 stimulates rat preantral follicle growth and also stimulates basal estradiol production in granulosa cells (17, 18). Thus, GDF-9 functions as a multipurpose oocyte-secreted growth factor during the early stages of folliculogenesis and in the periovulatory period.

Using a homology-based cloning strategy, we fortuitously cloned GDF-9 homologs from the mouse and human that we termed bone morphogenetic protein 15 (BMP-15) (19) [also called growth differentiation factor 9B (20)]. In addition to the 52% identity with GDF-9, BMP-15 had several interesting features. First, *Bmp15* mRNA was exclusively expressed in oocytes in an identical pattern as *Gdf9* (15, 19). Second, mouse *Bmp15* and human *BMP15* map to syntenic positions on the X chromosome. Third, similar to GDF-9, BMP-15 protein lacks the mature peptide cysteine that normally forms an intermolecular disulfide bond in the other TGFβ superfamily members. These findings suggest that BMP-15 and GDF-9 may directly interact (*i.e.* form heterodimers) or functionally interact (*i.e.* play redundant or antagonistic roles). Recent evidence from studies in sheep suggests interacting roles of these proteins in the ovary. The *BMP15* gene was cloned in sheep and shown to be mutated in *Inverdale* and *Hanna* sheep carrying the fecundity X (*FecX*^{I} and *FecX*^{H}) mutations (21). Both strains have mutations in the mature peptide sequence. Sheep heterozygous for these *BMP15* mutations show an increased ovulation frequency resulting in more twins and triplets. Surprisingly, sheep homozygous for these mutations are infertile and have a block in folliculogenesis that phenocopies the mouse *Gdf9* knockout ovarian phenotype. Thus, BMP-15 appears to be the second known oocyte-secreted growth factor that is critical for ovarian function.

In this report, we used the previously isolated mouse *Bmp15* gene sequences (19) to create male and female mice with a null mutation in the X-linked *Bmp15* gene. These *Bmp15* null female mice are viable but display reproductive defects. In addition, we have intercrossed these *Bmp15* null mice with mice carrying a mutation in the autosomal *Gdf9* gene to uncover genetic interactions. These knockout mouse models have helped us define the important roles of BMP-15 and GDF-9 in oocyte-somatic cell interactions during folliculogenesis and in the periovulatory period.

RESULTS

Targeted Mutation of the Bmp15 Gene in ES Cells and Generation of Bmp15 Null Mutant Mice

We had previously isolated the mouse *Bmp15* gene from a 129SvEv genomic library and shown that it was composed of two exons with a 3.5-kb intron. *Bmp15* exon 1 encodes the 17-amino acid signal peptide and 91 amino acids of the propeptide, whereas exon 2 encodes the remaining 159 amino acids of the propeptide and the 125-amino acid mature domain. To generate a mutant allele in the *Bmp15* gene in ES cells, we used the 129SvEv genomic sequences to construct a targeting vector to delete exon 2 (Fig. 1A). Recombination of this targeting vector and the endogenous *Bmp15* locus was anticipated to yield a null allele because no mature (active) BMP-15 could be synthesized if the gene sequences encoding it were deleted. A similar strategy had been employed to generate a null allele in the *Gdf9* locus (5).

The *Bmp15* targeting vector was electroporated into AB2.1 ES cells (XY), and 13 of 92 (14%) of the ES cell clones analyzed were targeted at the *Bmp15* locus and thereby null. Two of these ES cell lines were used to produce chimeric male mice that were fertile and transmitted the X-linked *Bmp15* null allele (*Bmp15*^{tm1Zuk} or *Bmp15*$^{-}$ or X^{Bmp15tm1}) to females. X^{Bmp15tm1}X (heterozygous or *Bmp15*$^{+/-}$) females were used to generate X^{Bmp15tm1}Y (null) males that were intercrossed with heterozygous females to produce X^{Bmp15tm1}X^{Bmp15tm1} (null or *Bmp15*$^{-/-}$) females (Fig. 1B, *top*). Using Southern blot analysis of DNA, a *Bmp15* exon 2 probe demonstrated a lack of a hybridizable signal in the DNA derived from X^{Bmp15tm1}Y and X^{Bmp15tm1}X^{Bmp15tm1} mice but not X^{Bmp15tm1}X or XY mice (Fig. 1B, *bottom*). This confirmed that the *Bmp15*^{tm1Zuk} allele is a null allele.

Fertility Analysis of Bmp15 Mutant Mice

Chimeric males, null males, heterozygous females, and null females were all viable and failed to demonstrate any gross developmental defects. In addition, male chimeric and *Bmp15* null males were fertile, and *Bmp15* null males had normal testis size [87.58 $\pm$ 2.42 ng/testis (n = 18)] compared with wild-type controls [87.27 $\pm$ 2.53 ng/testis (n = 11)]. The viability of *Bmp15* mutant mice and the fertility of the chimeric

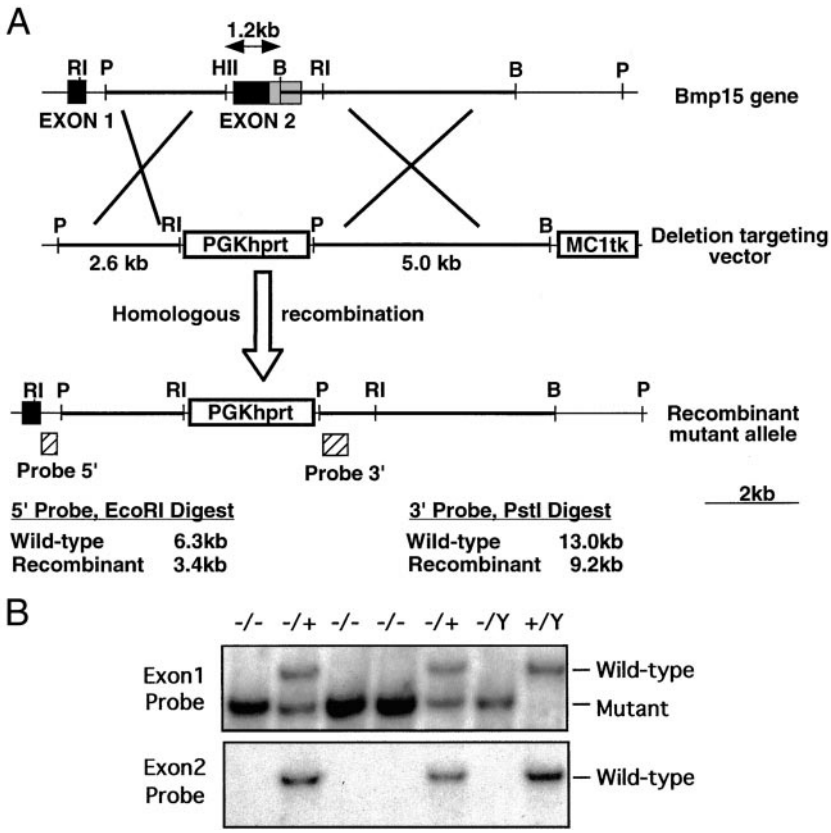

Fig. 1. Construct to Generate a *Bmp15* Mutant Allele in ES Cells and Generation of *Bmp15* Mutant Mice

A, The *Bmp15* replacement targeting vector to delete exon 2 is shown. The targeting vector was electroporated into hprt-deficient AB2.1 ES cells to produce the *Bmp15* recombinant mutant allele. The mutant allele can be distinguished from the wild-type allele using 5′- or 3′-probes as shown. B, Southern blot analysis of tail DNA derived from seven offspring from a litter from a mating of $X^{Bmp15tm1}Y$ and $X^{Bmp15tm1}X$ parents. Genomic DNA was digested with *Pst*I and analyzed as described previously (23) using the 3′-probe (*top panel*). The probe detects a 13.0-kb wild-type band in lanes derived from wild-type (+/Y) XY males and heterozygous (+/−) $X^{Bmp15tm1}X$ females and a 9.2-kb recombinant mutant band in lanes derived from null $X^{Bmp15tm1}Y$ (−/Y) males, heterozygous females, and null $X^{Bmp15tm1}X^{Bmp15tm1}$ (−/−) females. Southern blot analysis of the same DNA as in the *top panel* using an exon 2 probe (*bottom panel*) detects the 13.0-kb wild-type allele in DNA derived from the XY or $X^{Bmp15tm1}X$ offspring but not in the null males or females confirming the null status of the $Bmp15^{tm1Zuk}$ allele.

and null males are consistent with the limited adult ovary-specific expression of *Bmp15* mRNA (19).

To determine whether *Bmp15* plays a key ovarian function in females, heterozygous and homozygous mutant females were mated to males. In contrast to GDF-9, which is absolutely required for fertility in females, *Bmp15* homozygous mutants (C57/129 hybrid background) were subfertile when bred over a 1-yr period (Table 1). When the *Bmp15* mutation was maintained on a 129SvEv inbred background strain (in which females are normally less fertile), the *Bmp15* homozygous null females displayed a consistent (although more severe) subfertility compared with the *Bmp15* heterozygotes (Table 1). Both the number of pups per litter and the number of litters per month were reduced for the $Bmp15^{-/-}$ females from either hybrid or inbred genetic backgrounds. Thus, BMP-15 plays an important role in female reproduction in mice but is not as essential as GDF-9 or its sheep ortholog.

Ovarian and Oocyte Physiology

To determine the cause of the subfertility in the $Bmp15^{-/-}$ female mice, ovaries were analyzed both morphologically and histologically at various time points. In contrast to $Gdf9^{-/-}$ ovaries, which were extremely small (5), $Bmp15^{-/-}$ ovaries were often grossly indistinguishable from either $Bmp15^{+/-}$ or wild-type ovaries. Histological analysis of these mutant ovaries confirmed our gross impressions. In general, $Bmp15^{-/-}$ ovaries at all ages up through 1 yr demonstrated all stages of follicle development and multiple corpora lutea and appeared indistinguishable from control ovaries (Fig. 2). These findings would be consistent with the ability of $Bmp15^{-/-}$ mice to become pregnant. However, occasional $Bmp15^{-/-}$ ovaries at different ages demonstrated very few follicles and had an increased number of zona pellucida (ZP) remnants (data not shown; see below). Single rare

Table 1. Mating Data for *Bmp15* and *GDf9* Mutant Mice

Female Genotype	Genetic Background	No. of Females	Total Litters	Average Litter Size	Litters/ Month
$Bmp15^{+/-}$[a]	C57/129	9	100	7.42 ± 0.25	0.93
$Bmp15^{-/-}$	C57/129	13	112	4.93 ± 0.25	0.73
$Bmp15^{+/-}$	129	7	48	4.65 ± 0.33	0.77
$Bmp15^{-/-}$	129	6	20	2.95 ± 0.30	0.37
$Gdf9^{+/-}$	C57/129	7	78	9.88 ± 0.39	0.93
$Bmp15^{-/-}Gdf9^{+/-}$[b]	C57/129	21	93	3.67 ± 0.22	0.49
$Bmp15^{+/-}Gdf9^{+/-}$	129	15	64	4.39 ± 0.26	0.73
$Bmp15^{-/-}Gdf9^{+/-}$	129	12	0	0	0

C57/129 mice were bred for 1 yr; $Bmp15^{+/-}$ and $Bmp15^{-/-}$ 129 inbred mice were bred for 9 months; $Bmp15^{+/-}Gdf9^{+/-}$ and $Bmp15^{-/-}Gdf9^{+/-}$ 129 inbred mice were bred for 4–6 months.

[a] The fertility of $Bmp15^{+/-}$ mice is not statistically different compared to our wild-type female mice [8.4 ± 0.2 pups/litter, n = 107 (39), FSHβ heterozygotes [7.9 ± 0.3 pups/litter, n = 47 (our unpublished data)], or oxytocin heterozygotes [7.1 ± 0.3 pups/litter, n = 50 (Ref. 40 and unpublished data)].

[b] Four females died during the study, possibly secondary to parturition difficulties; four females were infertile.

$Bmp15^{-/-}$ and $Bmp15^{+/-}$ mice had unilateral or bilateral cysts at 1 yr of age. These findings have never been seen in wild-type mice in our laboratory.

Since $Bmp15^{-/-}$ ovarian histology was fairly normal, we subjected the $Bmp15^{+/-}$ and $Bmp15^{-/-}$ mice (C57/129 hybrid background) to a pharmacological superovulation protocol and determined the number of eggs that were ovulated. "Normal" numbers of eggs were released by the $Bmp15^{+/-}$ females (36.4 ± 3.7 eggs; n = 26 females), but $Bmp15^{-/-}$ females ovulated about two-thirds the number of oocytes as the controls (24.1 ± 3.0 eggs; n = 21 females). To uncover the cause of the reduced ovulations, we collected and analyzed ovaries from some of these superovulated mice. Whereas it was extremely difficult to find any oocytes inside follicles after the PMSG and hCG treatment in the case of the wild-type or $Bmp15^{+/-}$ females (Fig. 2E), $Bmp15^{-/-}$ ovaries occasionally had denuded oocytes that were larger than normal and had few cumulus cells surrounding the oocytes (Fig. 2F). These findings suggested that follicular recruitment and the number of preovulatory follicles were likely normal in the $Bmp15^{-/-}$ mice but that a percentage of the oocytes were trapped within follicles and were not released. A similar phenotype is also seen for the EP2 PGE_2 receptor knockout mice (22) whereas an absolute failure to ovulate is seen with cyclooxygenase 2 and progesterone receptor knockout mice (7, 8). In addition to these ovulation defects, $Bmp15^{-/-}$ mice also demonstrated a reduction of oocytes that could develop to embryos although $Bmp15^{+/-}$ oocytes also appeared to have some reduction compared with wild-type mice (Table 2; see below).

Analysis of Gdf9 and Bmp15 mRNA in Mutant Mice

One possibility for the defects in the *Gdf9* knockout mice is that there is altered regulation of *Bmp15* mRNA whereas the less severe phenotype of the *Bmp15* knockout mice could be due to increased compensation of GDF-9. To determine whether there were changes in the transcriptional regulation of *Bmp15* mRNA in *Gdf9* knockout ovaries or *vice versa*, we performed Northern blot analysis of RNA derived from control or mutant ovaries. *Gdf9* mRNA expression was identical in control and $Bmp15^{-/-}$ ovaries (Fig. 3). In contrast, *Bmp15* mRNA levels were higher in the $Gdf9^{-/-}$ ovary samples compared with control ovaries (Fig. 3). This relative increase in *Bmp15* mRNA was due to a dramatic increase in oocytes/unit volume in the $Gdf9^{-/-}$ ovaries (5). We have confirmed this by showing that four other oocyte-specific genes also show a relative increase in mRNA levels in the $Gdf9^{-/-}$ ovaries compared with wild-type ovaries (C. Yang, P. Wang, and M. M. Matzuk, unpublished data). Thus, the abnormalities in the *Gdf9* knockout ovaries are not due to transcriptional inactivation of the *Bmp15* gene nor is there a compensatory increase of *Gdf9* mRNA in the *Bmp15* knockout ovaries.

Characterization of $Bmp15^{-/-}Gdf9^{+/-}$ Double Mutant Mice

To study possible genetic, physical, and functional interactions between *Bmp15* and *Gdf9*, we intercrossed mice carrying the *Gdf9* null mutation (5) with the *Bmp15* null mutants generated herein. Initial studies focused on comparing the breeding of female mice homozygous for the *Bmp15* mutation and heterozygous for the *Gdf9* mutation ($Bmp15^{-/-}Gdf9^{+/-}$) to either $Gdf9^{+/-}$ or $Bmp15^{-/-}$ or $Bmp15^{+/-}$ mutant mice. Whereas $Gdf9^{+/-}$ mice appear to produce more offspring per litter than $Bmp15^{+/-}$ mice, similar litters per month were seen (Table 1). In contrast, the $Bmp15^{-/-}Gdf9^{+/-}$ females on a C57/129 background that gave birth produced even fewer pups per litter (3.67 ± 0.22) compared with the $Bmp15^{-/-}$ females (4.93 ± 0.25). Furthermore, the number of litters per month was further reduced to approximately half of the controls, and four females were com-

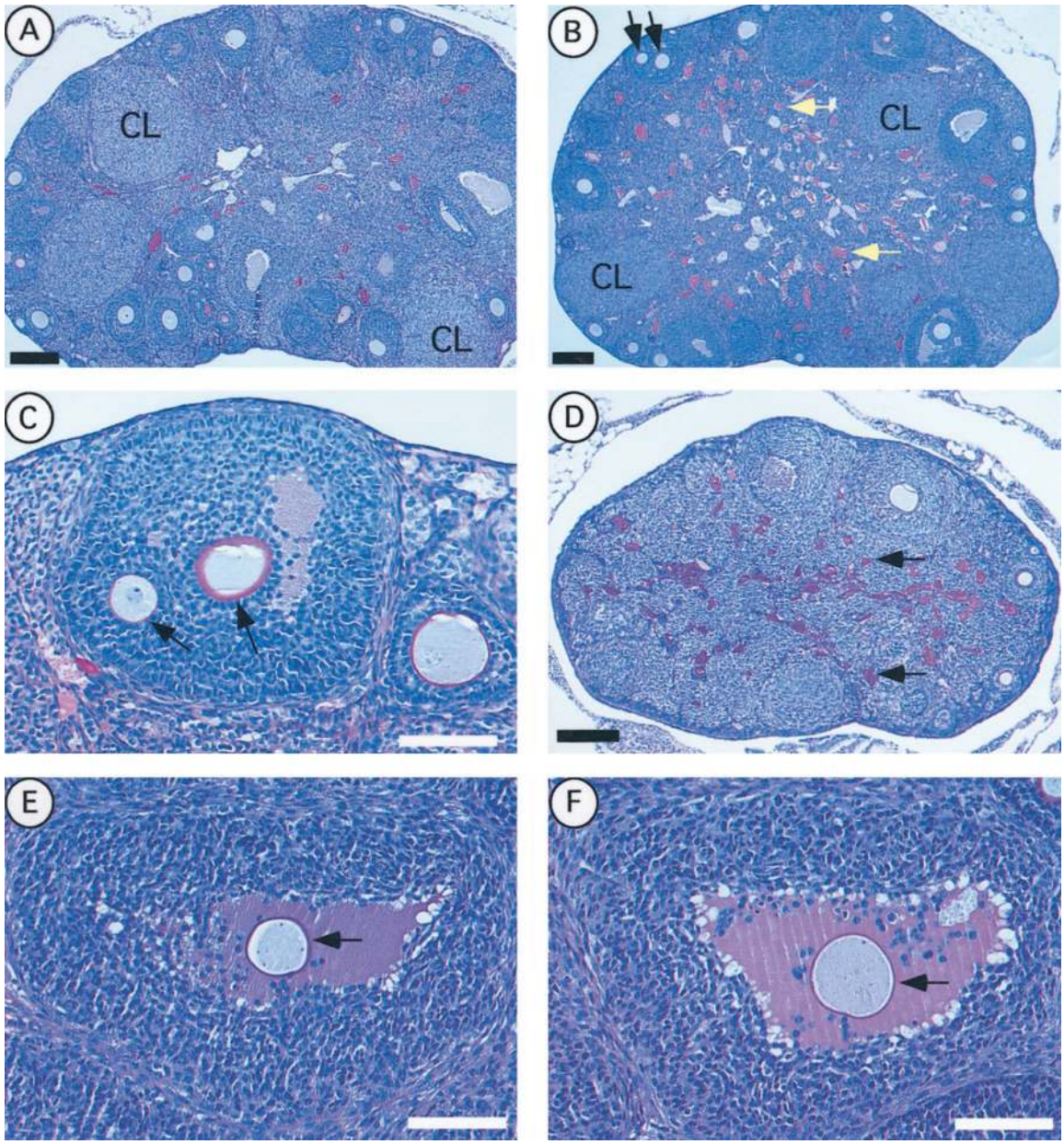

Fig. 2. Histological Analysis of *Bmp15* Mutant Ovaries

A, Ovary from a 4-month-old *Bmp15*$^{-/-}$ 129 mouse showing normal follicular development and corpora lutea (CL). B, Ovary from a 6-month-old *Bmp15*$^{+/-}$ 129 mouse showing normal follicular development and corpora lutea except there is a single follicle with two oocytes (*black arrows*) and accumulation of ZP remnants (*yellow arrows*). C, High-power magnification of a follicle with two oocytes from a 4-month-old *Bmp15*$^{-/-}$ 129 ovary. Additional examples of multiple oocytes in a single follicle were seen in double mutant mice (see below). D, Ovary from a 1-yr-old *Bmp15*$^{-/-}$ 129 mouse showing fairly normal follicular development and corpora lutea except for the accumulation of PAS-positive material (*arrows*) and ZP remnants in the interstitium. There is also a reduction in the number of oocytes and follicles compared with younger mice. E, Follicle with a small, trapped denuded oocyte (*arrow*) from a superovulated *Bmp15*$^{+/-}$ C57/129 mouse. F, Follicle with a large, trapped denuded oocyte (*arrow*) from a superovulated *Bmp15*$^{-/-}$ C57/129 mouse. All sections were stained with PAS/hematoxylin; for the *scale bars*, *white lines* represent 100 μm; *black lines* represent 200 μm.

pletely infertile. We also saw an increased incidence of death in these breeding *Bmp15*$^{-/-}$*Gdf9*$^{+/-}$ females (4 of 21 breeding females) but not in *Bmp15*$^{-/-}$*Gdf9*$^{+/-}$ females that were caged without males; we attribute these deaths to a failure to deliver singlets and subsequent intrauterine infection. Recent breeding of 129 inbred *Bmp15*$^{-/-}$*Gdf9*$^{+/-}$ females over a 6-month period failed to produce any offspring in contrast to the breeding of 129 inbred *Bmp15*$^{+/-}$*Gdf9*$^{+/-}$ females over a 4- to 6-month period, which yielded 64 litters (0.73 litters/month) with an average litter size of 4.39 (Table 1). These findings for the 129 inbred *Bmp15*$^{-/-}$*Gdf9*$^{+/-}$ females

Table 2. *In Vivo* "Fertilization" Data from Wild-Type and *Bmp15* and *Gdf9* Mutant Mice

Female Genotype	No. of Females	Embryos/Total Eggs	Percent "Fertilized"
Wild-type	12	34.25/36.83	93.0%
Gdf9$^{+/-}$	10	24.00/37.30	64.3%
Bmp15$^{+/-}$	14	23.50/37.79	62.2%
Bmp15$^{-/-}$	11	14.73/29.18	50.4%
Bmp15$^{-/-}$*Gdf9*$^{+/-}$	10	5.9/42.90	13.8%

All mice were C57/129 background and were mated to C57/129 stud male mice. All female mice were 3–4 weeks of age at the time of the PMSG injection. The number of embryos was determined after 24 h of *in vitro* culture.

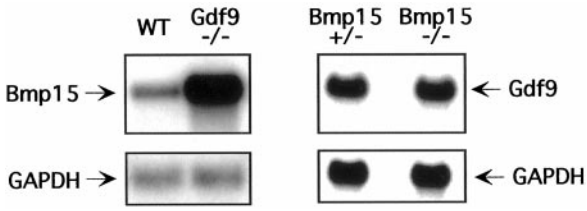

Fig. 3. Northern Blot Analysis of *Gdf9* and *Bmp15* in Control and Mutant Ovaries

Analysis of the expression of *Bmp15* mRNA in *Gdf9*$^{-/-}$ ovaries and controls (*top left*). Analysis of the expression of *Gdf9* mRNA in *Bmp15*$^{-/-}$ ovaries and controls (*top right*). Each blot was subsequently analyzed for expression of GAPDH mRNA as a control for RNA loading and integrity (*bottom panels*).

are even more dramatic than the *Bmp15*$^{-/-}$*Gdf9*$^{+/-}$ hybrid strain data and 129 inbred *Bmp15*$^{-/-}$ female mice that breed poorly. Thus, by reducing the dosage of these two related oocyte-expressed proteins, we have uncovered important genetic interactions.

To further understand the subfertility defects of the *Bmp15*$^{-/-}$*Gdf9*$^{+/-}$ females, we analyzed the ovaries histologically. Similar to the *Bmp15*$^{-/-}$ ovaries, normal folliculogenesis and corpora lutea could be observed in a minority of *Bmp15*$^{-/-}$*Gdf9*$^{+/-}$ ovaries up through 1 yr (Fig. 4, A and F). However, abnormalities were observed in five of nine ovaries from 6- to 7-month-old mice, three of five 9-month-old mice, and 12 of fourteen 11- to 12-month-old mice. These abnormalities included decreased numbers of late-stage follicles, increased oocyte loss, and increased ZP remnants, accumulation of periodic acid Schiff (PAS)-positive material in the interstitium, follicles with multiple oocytes, and absence of corpora lutea (Fig. 4, B and C). This progressed to the point where there were very few oocytes and follicles in some ovaries by 1 yr of age (Fig. 4G). Thus, these findings suggest that BMP-15 and GDF-9 play synergistic roles in oocyte survival and folliculogenesis.

To follow up on some of the above findings, we performed immunohistological analysis of the ovaries that contained prominent PAS-positive (magenta-colored) structures, which resembled ZP after oocyte degeneration. These structures are a prominent finding in the GDF-9-deficient mice. Ovaries from five independent mice presented in Figs. 4 and 7 were analyzed using antibodies specific for ZP protein 1 (ZP1), 2 (ZP2), or 3 (ZP3) or a nonspecific antibody. Antibodies to ZP1, ZP2, or ZP3 stained the ZP around intact oocytes and also detected the prominent remnants centrally (Fig. 5, A–C), confirming that these are remnants of ZP after the oocyte had disappeared. The nonspecific antibody failed to detect any signal in the ovaries (Fig. 5D) confirming the specificity of the anti-ZP antibodies. These ZP remnants appear to be quite stable after oocyte loss (see below).

It was also a surprise to find follicles that contained multiple oocytes (Fig. 4, D and E). To quantitatively study these findings, we analyzed multiple adjacent sections (8–10 sections per pair of ovaries) of 129SvEv inbred ovaries from *Bmp15*$^{-/-}$*Gdf9*$^{+/-}$ *vs.* *Bmp15*$^{+/-}$*Gdf9*$^{+/-}$ mice (littermate controls). Whereas only two of eight *Bmp15*$^{+/-}$*Gdf9*$^{+/-}$ mice contained follicles with multiple oocytes (two follicles total), four of eight *Bmp15*$^{-/-}$*Gdf9*$^{+/-}$ mice contained multiple oocytes (eight follicles total). Interestingly, two *Bmp15*$^{-/-}$*Gdf9*$^{+/-}$ mice and one *Bmp15*$^{+/-}$*Gdf9*$^{+/-}$ mouse had follicles with three oocytes in the follicle (Fig. 4E). These findings are rare for wild-type inbred 129SvEv mice. Thus, the dosage of these ligands appears to somehow alter the development of the granulosa cell layers around individual oocytes, allowing the formation of these double and triple oocyte follicles.

Since folliculogenesis was relatively normal in the *Bmp15*$^{-/-}$*Gdf9*$^{+/-}$ ovaries at early time points, we analyzed the ability of the *Bmp15*$^{-/-}$*Gdf9*$^{+/-}$ oocytes to be pharmacologically released and fertilized *in vivo*. Whereas the *Bmp15*$^{-/-}$*Gdf9*$^{+/-}$ mice had high numbers of oocytes released (Table 2), only 13.8% of these oocytes developed to embryos. Analysis of eggs from *Bmp15*$^{-/-}$*Gdf9*$^{+/-}$ females that were subjected to PMSG/hCG treatment but were not mated with males revealed the likely cause of the *Bmp15*$^{-/-}$*Gdf9*$^{+/-}$ defects. Normally, cumulus cell-egg complexes from wild-type and *Gdf9*$^{+/-}$ mice demonstrate a resilient adhesion of cumulus cells and eggs upon removal of the complexes from the oviduct (Fig. 6A). In contrast, cumulus cells fail to adhere to eggs isolated from the oviducts of *Bmp15*$^{-/-}$*Gdf9*$^{+/-}$ mutant mice (Fig. 6B). A similar finding was also seen for many of the cumulus cell-egg complexes isolated from *Bmp15*$^{-/-}$ mice. Furthermore, treatment of immature *Bmp15*$^{-/-}$*Gdf9*$^{+/-}$ mice with PMSG for 48 h and subsequent analysis of their ovaries 8 h after hCG injection revealed the presence of some follicles in which cumulus expansion had not occurred or examples of large denuded oocytes (oocytes that were completely lacking cumulus cells) (Fig. 4I). This finding was in contrast to *Gdf9*$^{+/-}$ mice (Fig. 4H). Analysis of individual sections of ovaries from wild-type or *Gdf9*$^{+/-}$ ovaries revealed 25 preovulatory follicles in which cumulus expansion appeared normal and 29 oocytes of antral follicles that were appropriate in size (11). However, anal-

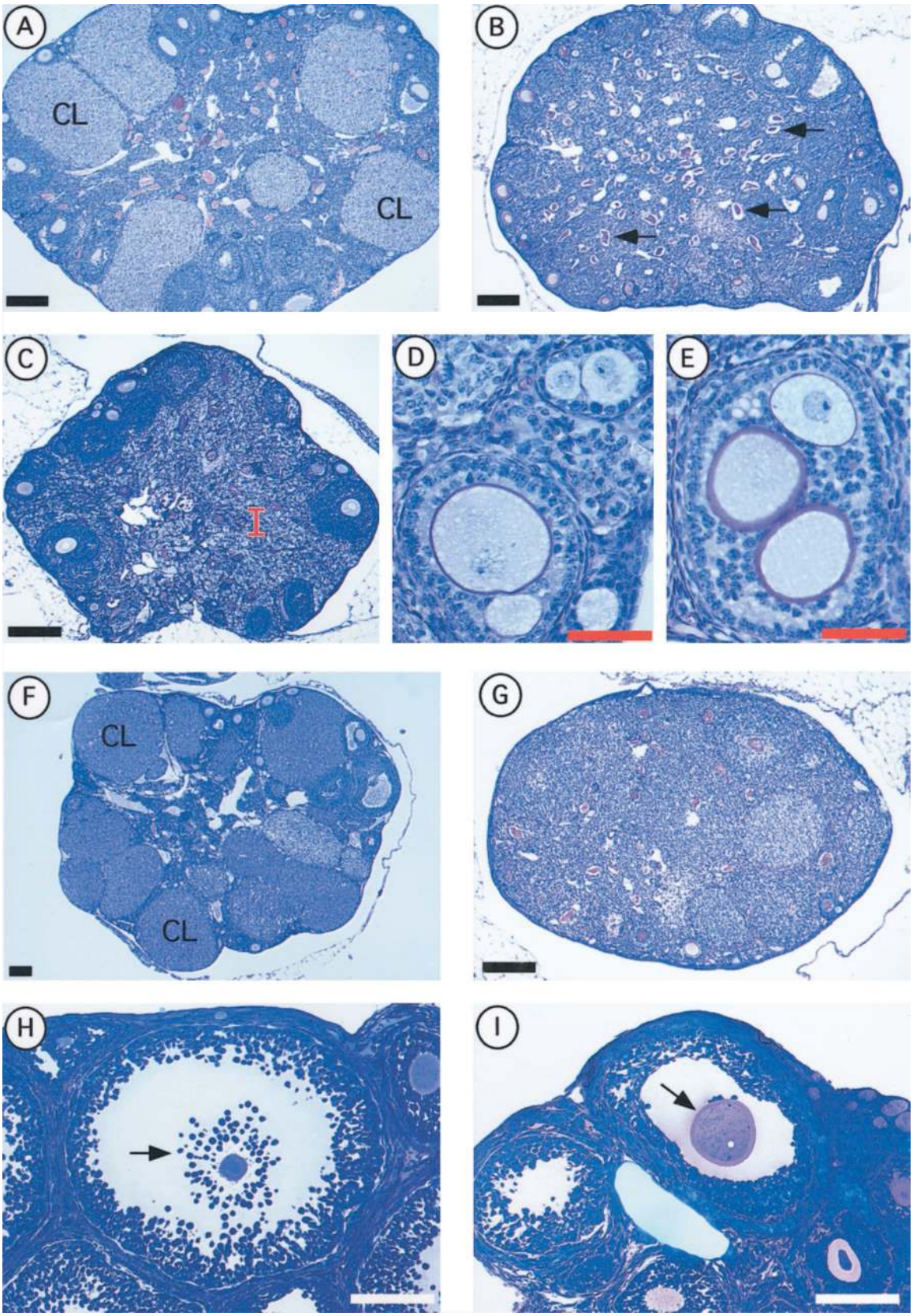

Fig. 4. Histological Analysis of *Bmp15*$^{-/-}$*Gdf9*$^{+/-}$ Ovaries and *Gdf9*$^{+/-}$ Control Ovary

A–F, *Bmp15*$^{-/-}$*Gdf9*$^{+/-}$ ovaries at 6 months (A–C), 4 months (D and E), 1 yr (F), and 10 months (G). Normal folliculogenesis and corpora lutea (CL) are seen in two of these ovaries (A and F). Abnormalities in folliculogenesis, a decrease in number of

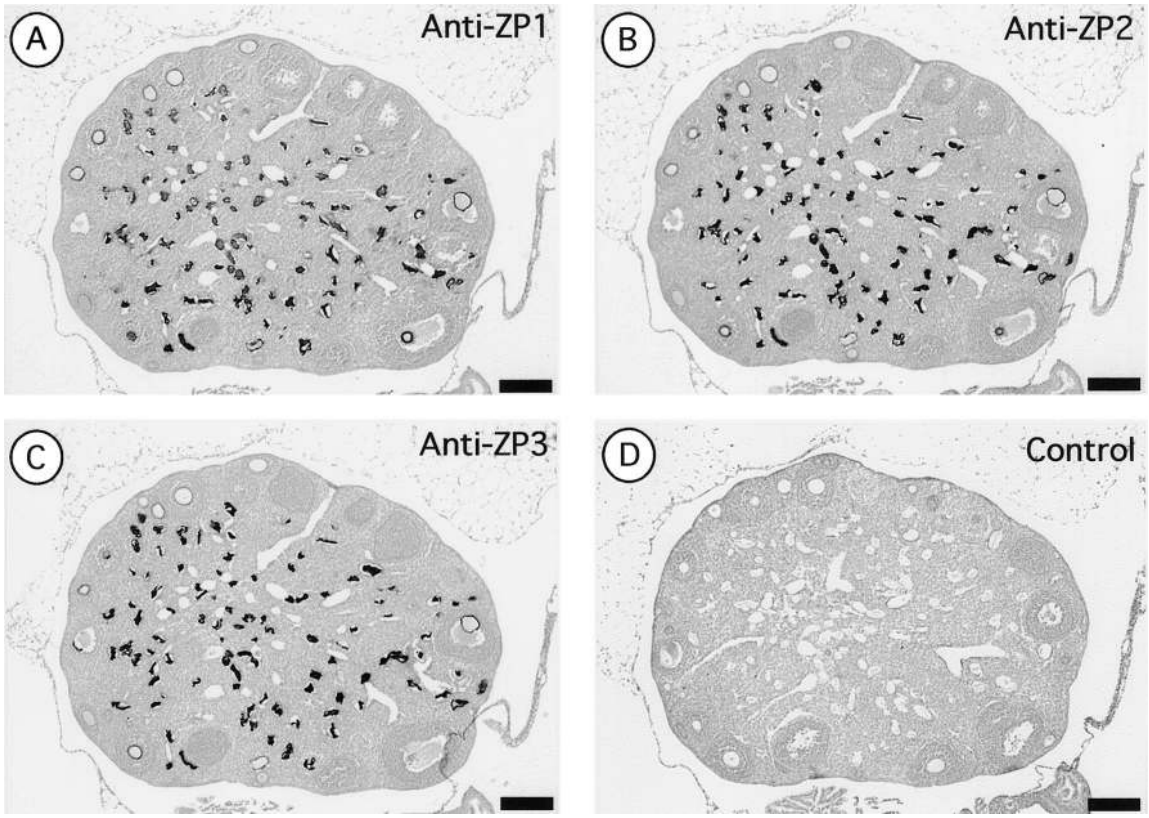

Fig. 5. Immunohistological Analysis of ZP Proteins

The *Bmp15*$^{-/-}$*Gdf9*$^{+/-}$ ovary shown in Fig. 4B was analyzed with polyclonal antibodies to ZP1 (A), ZP2 (B), ZP3 (C), and a nonspecific (control) antibody (D). Both ZP around intact oocytes around the periphery and the ZP remnants centrally after oocyte loss are detected (*dark staining*) with all three antibodies but not the nonspecific antibody. The sections were counterstained with hematoxylin. The *black scale bars* represent 200 μm.

ysis of *Bmp15*$^{-/-}$ or *Bmp15*$^{-/-}$*Gdf9*$^{+/-}$ ovaries revealed 11 of 19 antral follicles where absence of cumulus expansion had occurred or where oocytes were larger than normal in size. In addition to these findings, there was one case in which the cumulus granulosa cells were seen invading the ZP. These findings were not unique to pharmacologically treated mice but were also observed in seven of ten 11- to 12-month-old *Bmp15*$^{-/-}$*Gdf9*$^{+/-}$ mice in which denuded oocytes in antral follicles (total of seven oocytes with cumulus cell defect) and oocytes trapped in corpora lutea (total of eight trapped oocytes) were observed. Six of six *Bmp15*$^{+/-}$ mice of the same age failed to demonstrate these defects. We believe that these findings are part of the variation in the cumulus cell adhesion/oocyte-cumulus cell interaction phenotype. Thus, these studies demonstrate that BMP-15 and GDF-9 play functionally redundant roles in cumulus expansion and maintenance of a cohesive interaction between cumulus cells and oocytes or eggs that influences subsequent fertility.

Production of Mice Null for Both Bmp15 and Gdf9

One possible reason for the early block in folliculogenesis in the *Gdf9* knockout mice could be due to persistent (unopposed) BMP-15 protein levels since the *Bmp15* mRNA continued to be expressed in these mice. Thus, to ensure that the *Gdf9* knockout phenotype was due to absence of GDF-9 and not secondary to unopposed BMP-15, mice lacking both BMP-15

corpora lutea, interstitial cell proliferation (I), increased oocyte loss, and multiple ZP remnants (*arrows*) are seen in the other sections from independent mice (B, C, and G). Follicles with multiple oocytes are also seen (D and E). In panel D, two small oocytes are seen (*top right*) as well as two other oocytes of differing sizes (*bottom left*) surrounded by a complete layer of granulosa cells and basement membrane. In panel E, three similar size oocytes are surrounded by a single granulosa cell layer. H and I, Treatment of *Gdf9*$^{+/-}$ (H) and *Bmp15*$^{-/-}$*Gdf9*$^{+/-}$ (I) immature mice with PMSG (48 h) and hCG (8 h) revealed normal cumulus expansion of the granulosa cells in the control (H, *arrow*) but an absence of cumulus cells around a large oocyte (*arrow*) in the *Bmp15*$^{-/-}$*Gdf9*$^{+/-}$ mutant (I). Sections A–G were stained with PAS/hematoxylin. Sections H and I were stained with toluidine blue. For the *scale bars*, the *red lines* represent 50 μm, the *white lines* represent 100 μm, and the *black lines* represent 200 μm. The diameter of the "fixed" oocyte in panel I is 65 μm.

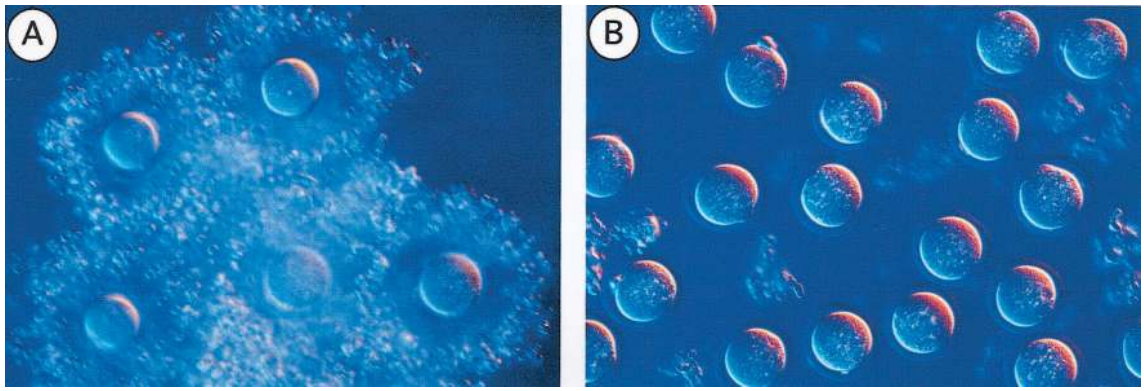

Fig. 6. Eggs Isolated from *Gdf9*$^{+/-}$ (A) and *Bmp15*$^{-/-}$*Gdf9*$^{+/-}$ (B) Mutant Mice

Eggs isolated from the oviducts of *Gdf9*$^{+/-}$ females after PMSG and hCG stimulation were embedded in a resilient three-dimensional extracellular matrix which contained cumulus cells (A). In contrast, the cumulus cells of *Bmp15*$^{-/-}$*Gdf9*$^{+/-}$ mice were loosely attached to the oocyte and readily fell off the oocyte (B). Eggs were isolated from C57/129 hybrid strain mice.

and GDF-9 (*i.e. Bmp15*$^{-/-}$*Gdf9*$^{-/-}$) mice were generated. At early time points, the ovaries of these *Bmp15*$^{-/-}$*Gdf9*$^{-/-}$ mice resembled the ovaries of *Gdf9*$^{-/-}$ mice and demonstrated a block at the type 3B primary (one-layer) follicle stage (Fig. 7B). Furthermore, similar to *Gdf9*$^{-/-}$ mice, unilateral and bilateral cysts were grossly (Fig. 7A) and microscopically (Fig. 7E) present. Only one cyst per ovary was present in these double mutant mice as in the *Gdf9*$^{-/-}$ mice. At later time points, there were a number of unique abnormalities found in the *Bmp15*$^{-/-}$*Gdf9*$^{-/-}$ ovaries. These abnormalities included increased loss of oocytes, increased ZP remnants, complete absence of oocytes, and proliferation of cells in the interstitium (sometimes PAS-positive) (Fig. 7, C–F), and a rare mouse that displayed a transformation of the granulosa cells into Sertoli-like cells (Fig. 7, G and H) similar to mice lacking inhibin α (23) or estrogen receptors α and β (24). Interestingly, accumulation of ZP remnants are seen after loss of oocytes in the *Gdf9*$^{-/-}$ ovaries (5) but are not seen after loss of oocytes in animal models that have blocks at later stages such as FSHβ, cyclooxygenase 2, or progesterone receptor knockouts (6–8). It is not clear whether there are altered proteolytic processing defects in the ovaries of mice that have blocks at the primary follicle stage *vs.* blocks at later stages. Thus, unopposed BMP-15 is not the cause of the *Gdf9* knockout phenotype but BMP-15 appears to play some additional roles along with GDF-9 in oocyte survival.

DISCUSSION

We have used knockout mouse technology and genetic intercrosses to define the functions of BMP-15 and its interactions with GDF-9. Our studies have uncovered periovulatory functions of BMP-15 in females and confirm our *in vitro* studies (13, 15, 16) by showing that GDF-9 also plays a key role in this period. We have demonstrated that hybrid and inbred *Bmp15* knockout mice are subfertile due to reduced ovulation and fertilization; *Bmp15*$^{-/-}$*Gdf9*$^{+/-}$ mice demonstrate further defects in early follicle development compared with *Bmp15*$^{-/-}$ or *Gdf9*$^{+/-}$ mice. Previous studies had demonstrated an important role of oocyte-secreted proteins in cumulus expansion, hyaluronic acid synthesis signaling through the PGE_2 receptor EP2, and suppression of urokinase plasminogen activator and LH receptor (25). Furthermore, cumulus-oocyte complexes are known to synthesize progesterone and PGE_2. Using recombinant GDF-9, we have shown that GDF-9 can perform all of the functions of the oocyte-secreted protein(s) and also stimulate PGE_2 through an induction of cyclooxygenase 2 in cumulus cells and progesterone via induction of PGE_2 and the EP2 receptor. Our *in vivo* studies confirm these *in vitro* analyses; oocytes from *Bmp15*$^{-/-}$*Gdf9*$^{+/-}$ fail to demonstrate a stable "adherence" of cumulus cells likely due to a reduction of key periovulatory factors (*e.g.* hyaluronic acid and PGE_2). *Bmp15*$^{-/-}$*Gdf9*$^{+/-}$ mice also have some of the features of the progesterone receptor and cyclooxygenase 2 knockout mice [*i.e.* failure to release oocytes and the presence of oocytes trapped in corpora lutea (7, 8)], further confirming the *in vivo* relationship of these factors. Since *Gdf9*$^{+/-}$ mice do not demonstrate these defects and some *Bmp15*$^{-/-}$ mice demonstrate some of these defects, these findings also indicate an important role of BMP-15 in at least some of these processes.

Gdf9$^{-/-}$ and *Bmp15*$^{-/-}$*Gdf9*$^{-/-}$ mice develop unilateral and bilateral cysts with high frequency (Ref. 5 and the current study). These cysts can become very large (Fig. 7), and analysis of the cystic ovaries of these mice or after regression of the cysts demonstrates a dramatic reduction in the number of oocytes (*i.e.* the cysts lead to decreased oocyte survival). We believe that these findings in our knockout mice have important implications in humans. Polycystic ovarian syndrome (PCOS) is a major cause of reduced fertility in

women, and our findings suggest that the presence of cysts in the ovaries of these women could likewise lead to increased oocyte loss through direct structural destruction or via indirect growth factor/hormonal effects.

Unlike *Bmp15*$^{+/-}$ mice, *BMP15* heterozygous mutant sheep demonstrate increased fertility (*i.e.*, increased twins and triplets), suggesting that the BMP-15 propeptide sequences (present as the sheep mutations are in the mature peptide encoding region) are acting in a dominant negative fashion. This BMP-15 propeptide may be somehow interfering with GDF-9 homodimer, BMP-15 homodimer, and/or GDF-9/BMP-15 heterodimer formation. For example, the BMP-15 propeptide may preferentially bind to a wild-type GDF-9 propeptide monomer to cause decreased BMP-15/GDF-9 heterodimers and shift the equilibrium toward increased BMP-15 homodimers.

Interestingly, sheep homozygous for null mutations in the *BMP15* gene do not phenocopy *Bmp15* knockout mice but instead resemble *Gdf9*$^{-/-}$ mice (*i.e.* homozygotes are infertile due to a block at the primary follicle stage). How might one explain these findings? Based on the available animal models and *in vitro* studies, two different models could be evoked to explain the functions of GDF-9 and BMP-15 in sheep *vs.* mice (Fig. 8). In model A (the mouse model), GDF-9 homodimers would be the most bioactive and play the major function. This model is based on our findings from *Gdf9*$^{-/-}$ mice (5, 11, 12), which display an early block in folliculogenesis, and also on the present study on the *Bmp15*$^{-/-}$ mice (which have a defect in late folliculogenesis and ovulation). Furthermore, mouse GDF-9 homodimers, but not mouse BMP-15 homodimers, are active in our mouse *in vitro* bioassays (13, 16). A similar situation has been shown recently by our group in the case of the activin βA and βB monomers (26); using a gene "knockin" strategy, we demonstrated that activin βB (which shows 63% amino acid identity in the mature peptide sequence) can replace activin βA for some, but not all, functions, demonstrating that βB is less bioactive than βA. However, in model B (the sheep model), BMP-15 homodimers would be postulated to be the most bioactive compared with either GDF-9 homodimers or BMP-15/GDF-9 heterodimers. This model would explain how the sheep *BMP15* homozygous mutant phenotype mimics the *Gdf9*$^{-/-}$ mouse ovarian phenotype. Interestingly, mouse and sheep GDF-9 proteins are highly conserved whereas mouse and sheep BMP-15 proteins have diverged greatly (78% amino acid identity). Thus, it is possible that this protein divergence has altered the biopotency of these proteins, allowing BMP15 to become the more essential protein in sheep. Although these models assume signaling of the ligands through the same receptor, we cannot rule out evolutionary divergence of a common GDF-9 or BMP-15 receptor (or multiple receptors) to permit higher affinity interaction of the sheep receptor with BMP-15 homodimers to explain the *in vivo* findings. However, recent studies demonstrate that recombinant human BMP-15 stimulates *in vitro* rat granulosa cell proliferation and decreases FSH-induced progesterone production (27). This finding suggests that the BMP-15 receptors are conserved between species. Future structure-function and receptor binding studies should help us clarify the active forms of these ligands in the different mammalian species and determine whether BMP-15, GDF-9, or both are essential for human fertility.

MATERIALS AND METHODS

ES Cell Technology and Southern Blot Analysis

More than 20 kb of genomic sequence encompassing the two-exon mouse *Bmp15* gene were isolated from a 129SvEv genomic library (19). These genomic sequences were used to construct a targeting vector to mutate the *Bmp15* gene in ES cells. The targeting vector contained 2.6 kb of *Bmp15* intron 1 sequence, a positive selectable marker (the PGK-hprt expression cassette), 5.0 kb of sequence 3′ to the coding portion of exon 2, and a negative selectable marker [the MC1-tk (thymidine kinase) expression cassette (Fig. 1A)]. Linearized vector was electroporated into the hprt-negative AB2.1 ES cell line, cell clones were selected in HAT (hypoxanthine, aminopterine, and thymidine) and FIAU [1-(2′-deoxy-2′fluoro-β-D-arabinofuranosyl)-5-iodouracil], and DNA from the clones analyzed by Southern blot and targeted ES cell clones were expanded and injected into blastocysts as described previously (23, 28, 29). Fourteen percent of the ES cell clones were targeted at the *Bmp15* locus (data not shown), and two of these ES cell clones (*Bmp15*-79-D7 and *Bmp15*-79-F7), which were injected into blastocysts, produced male chimeras that successfully transmitted the mutant *Bmp15*^{tm1Zuk} allele to F_1 female offspring. F_1 and F_2 female heterozygotes and F_2 null male offspring were intercrossed to produce *Bmp15* null homozygotes. Chimeras were either bred to C57BL6/J females to produce 129SvEv/C57BL6/J hybrid mice or to 129SvEv females to produce 129SvEv inbred mice. Southern blot analysis was used for genotype analysis of all *Bmp15* mutant offspring as shown (Fig. 1B) and all *Gdf9* mutant offspring as described (5).

Breeding Experiments

Bmp15 heterozygous and homozygous mutant females from both hybrid (129SvEv/C57BL6J) and inbred (129SvEv) genetic backgrounds were bred to males of the same genetic backgrounds at 6 weeks of age and breeding was continued for up to 1 yr. To generate the *Bmp15*/*Gdf9* double mutant mice, mice carrying the *Gdf9*^{tm1Zuk} mutation (5) on either hybrid or 129SvEv inbred genetic backgrounds were bred to *Bmp15* mutant mice of similar genetic backgrounds. Breeding of the double mutants was also initiated at 6 weeks of age.

Immunohistological Analysis

Immunohistological analysis was carried out using epitope-selected antibodies purified from antisera of rabbits immunized with porcine ZP proteins as previously described (30, 31). To select ZP1-, 2-, and 3-specific antibodies that would recognize mouse ZP proteins, we used an epitope selection

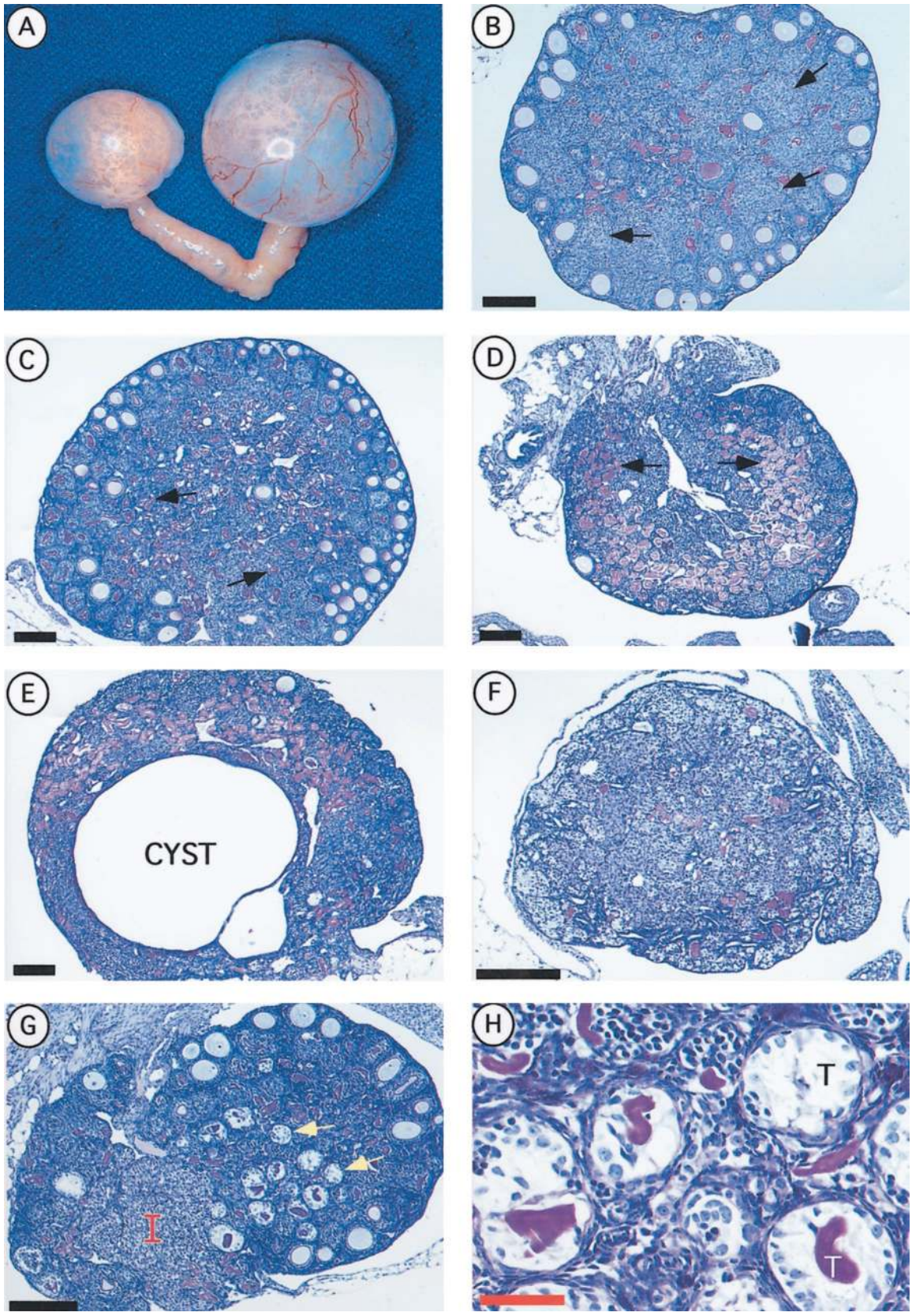

Fig. 7. Morphological and Histological Analysis of *Bmp15*$^{-/-}$*Gdf9*$^{-/-}$ Ovaries (A–H)

A, Morphological analysis of large bilateral cysts (1 cm and 1.7 cm) attached to the uterine horns of a 1-yr-old *Bmp15*$^{-/-}$*Gdf9*$^{-/-}$ mouse. B, Ovary from a 5-month-old mouse showing primary (type 3) follicles around the periphery and

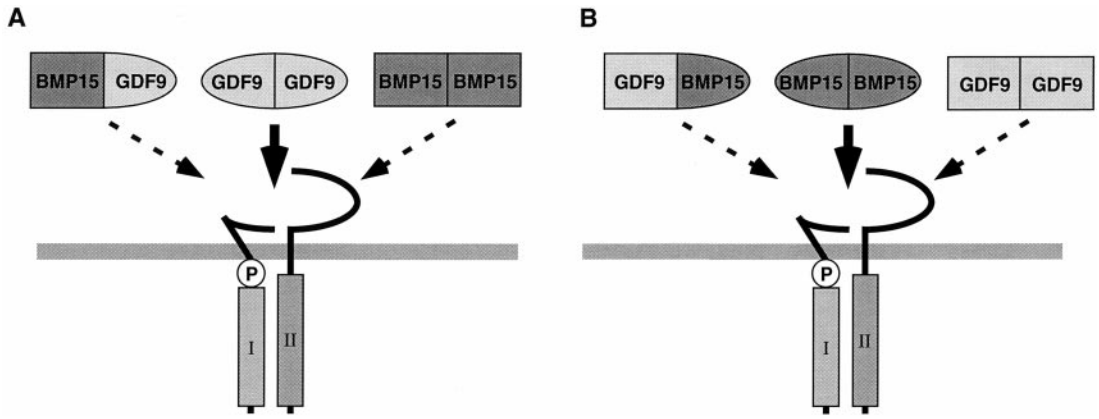

Fig. 8. Models for the Differential Functions of BMP-15 and GDF-9 in Mammals

A, In mice, GDF-9 homodimers appear to be the major signaling protein, whereas BMP-15 homodimers and BMP-15/GDF-9 heterodimers appear to play synergistic roles in the ovary. B, In sheep, BMP-15 homodimers play a major role although we cannot rule out significant roles of GDF-9 homodimers or BMP-15/GDF-9 heterodimers. In sheep, a model in which BMP-15/GDF-9 heterodimers are the active form could also explain the findings. We have shown that mouse and human BMP-15/GDF-9 heterodimers can form *in vitro* (N. Wolfman, unpublished data; P. Wang and M. M. Matzuk, unpublished data). Other members of the TGFβ superfamily can also form heterodimers that are more potent than the respective homodimers [*e.g.* heterodimers between the BMP-2/4 subgroup and the BMP-5/6/7 subgroup (36–38)].

method to enhance for cross-species ZP epitopes. Antibodies recognizing all three porcine ZP proteins were epitope selected using human ZP proteins made from cDNAs expressed using the baculovirus expression system (32, 33). Briefly, antibodies were incubated with each of the three human ZP proteins that had been isolated from SF9 insect cell lines. The individual proteins were transferred to polyvinylidenefluoride (PVDF) membrane and incubated with antiserum. Nonspecific antibodies were washed from the membrane and ZP-specific antibodies were eluted with 200 mM glycine buffer, pH 2.7, which was neutralized to pH 7. Antibody specificity to each of the ZP proteins was demonstrated by SDS-PAGE and immunoblot analysis as previously described (32, 34, 35).

Other Methods

RNA isolation, Northern blot analysis, histological analysis, pharmacological superovulation, and statistical methods were performed as described previously (5, 6, 12, 13, 19) and have been described briefly in the body of the text or the figure legends.

Acknowledgments

We thank Ms. Shirley Baker for aid in manuscript preparation and Dr. Hua Chang for help with the figures.

Received January 5, 2001. Revision received February 23, 2001. Accepted March 16, 2001.

Address requests for reprints to: Martin M. Matzuk, M.D., Ph.D., Department of Pathology, Baylor College of Medicine, One Baylor Plaza, Houston, Texas 77030. E-mail: mmatzuk@bcm.tmc.edu.

These studies were supported in part by the NIH Specialized Cooperative Centers Program in Reproduction Research (Grant HD-07495) and NIH Grant HD-33438 (to M.M.M.).

REFERENCES

1. Elvin JA, Matzuk MM 1998 Mouse models of ovarian failure. Rev Reprod 3:183–195
2. Elvin JA, Matzuk MM 2001 Control of ovarian function. In: Matzuk MM, Brown CW, Kumar TR (eds) Transgenics in Endocrinology. The Humana Press, Totowa, NJ, in press
3. Ruggiu M, Speed R, Taggart M, McKay SJ, Kilanowski F, Saunders P, Dorin J, Cooke HJ 1997 The mouse *Dazla* gene encodes a cytoplasmic protein essential for gametogenesis. Nature 389:73–76
4. Soyal SM, Amleh A, Dean J 2000 FIG(α), a germ cell-specific transcription factor required for ovarian follicle formation. Development 127:4645–54
5. Dong J, Albertini DF, Nishimori K, Kumar TR, Lu N, Matzuk MM 1996 Growth differentiation factor-9 is required during early ovarian folliculogenesis. Nature 383: 531–535
6. Kumar TR, Wang Y, Lu N, Matzuk MM 1997 Follicle stimulating hormone is required for ovarian follicle maturation but not male fertility. Nat Genet 15:201–204
7. Dinchuk JE, Car BD, Focht RJ, Johnston JJ, Jaffee BD, Covington MB, Contel NR, Eng VM, Collins RJ, Czerniak

follicular nests that resemble small corpora lutea (*arrows*) in the center. The phenotype of this ovary resembles the findings seen in *Gdf9*$^{-/-}$ ovaries (5, 12). C, Ovary from a 4-month-old mouse showing increased *magenta*-colored ZP remnants (*arrows*) throughout the center, a sign of increased oocyte turnover. D, Ovary from a 9-month-old showing few oocytes and a further accumulation of ZP remnants (*arrows*). E, Ovary from a 9-month-old mouse showing a central cyst, few oocytes, and increased ZP remnants. F, Ovary from a 1-yr-old mouse showing absence of oocytes. G and H, Low power (G) and high power (H) views of an ovary from a 4-month-old mouse showing multiple follicles (*arrows*) that resemble seminiferous tubules (T) with Sertoli-like cells. There is also interstitial (I) cell proliferation. All ovaries are derived from C57/129 hybrid mice. For the *scale bars*, the *red line* represents 50 μm, and the *black lines* represent 200 μm.

PM, Gorry SA, Trzaskos JM 1995 Renal abnormalities and an altered inflammatory response in mice lacking cyclooxygenase II. Nature 378:406–409
8. Lydon JP, DeMayo FJ, Funk CR, Mani SK, Hughes AR, Montgomery CA, Shyamala G, Conneely OM, O'Malley BW 1995 Mice lacking progesterone receptor exhibit pleiotropic reproductive abnormalities. Genes Dev 9:2266–2278
9. Tong ZB, Gold L, Pfeifer KE, Dorward H, Lee E, Bondy CA, Dean J, Nelson LM 2000 Mater, a maternal effect gene required for early embryonic development in mice. Nat Genet 26:267–268
10. Besmer P, Manova K, Duttlinger R, Huang EJ, Packer A, Gyssler C, Bachvarova RF 1993 The *kit*-ligand (steel-factor) and its receptor c-*kit*/*W*: pleiotropic roles in gametogenesis and melanogenesis. Development 119S: 125–137
11. Carabatsos MJ, Elvin JA, Matzuk MM, Albertini DF 1998 Characterization of oocyte and follicle development in growth differentiation factor-9-deficient mice. Dev Biol 203:373–384
12. Elvin JA, Yan C, Wang P, Nishimori K, Matzuk MM 1999 Molecular characterization of the follicle defects in the growth differentiation factor-9-deficient ovary. Mol Endocrinol 13:1018–1034
13. Elvin JA, Clark AT, Wang P, Wolfman NM, Matzuk MM 1999 Paracrine actions of growth differentiation factor-9 in the mammalian ovary. Mol Endocrinol 13:1035–1048
14. McGrath SA, Esquela AF, Lee S-J 1995 Oocyte-specific expression of growth/differentiation factor-9. Mol Endocrinol 9:131–136
15. Elvin JA, Yan C, Matzuk MM 2000 Oocyte-expressed TGF-β superfamily members in female fertility. Mol Cell Endocrinol 159:1–5
16. Elvin JA, Yan C, Matzuk MM 2000 Growth differentiation factor-9 stimulates progesterone synthesis in granulosa cells via a prostaglandin E2/EP2 receptor pathway. Proc Natl Acad Sci USA 97:10288–10293
17. Hayashi M, McGee EA, Min G, Klein C, Rose UM, van-Duin M, Hsueh AJW 1999 Recombinant growth differentiation factor-9 (GDF-9) enhances growth and differentiation of cultured early ovarian follicles. Endocrinology 140:1236–1244
18. Vitt UA, Hayashi M, Klein C, Hsueh AJ 2000 Growth differentiation factor-9 stimulates proliferation but suppresses the follicle-stimulating hormone-induced differentiation of cultured granulosa cells from small antral and preovulatory rat follicles. Biol Reprod 62:370–377
19. Dube JL, Wang P, Elvin J, Lyons KM, Celeste AJ, Matzuk MM 1998 The bone morphogenetic protein 15 gene is X-linked and expressed in oocytes. Mol Endocrinol 12: 1809–1817
20. Laitinen M, Vuojolainen K, Jaatinen R, Ketola I, Aaltonen J, Lehtonen E, Heikinheimo M, Ritvos O 1998 A novel growth differentiation factor-9 (GDF-9) related factor is co-expressed with GDF-9 in mouse oocytes during folliculogenesis. Mech Dev 78:135–140
21. Galloway SM, McNatty KP, Cambridge LM, Laitinen MP, Juengel JL, Jokiranta TS, McLaren RJ, Luiro K, Dodds KG, Montgomery GW, Beattie AE, Davis GH, Ritvos O 2000 Mutations in an oocyte-derived growth factor gene (BMP15) cause increased ovulation rate and infertility in a dosage-sensitive manner. Nat Genet 25:279–283
22. Hizaki H, Segi E, Sugimoto Y, Hirose M, Saji T, Ushikubi F, Matsuoka T, Noda Y, Tanaka T, Yoshida N, Narumiya S, Ichikawa A 1999 Abortive expansion of the cumulus and impaired fertility in mice lacking the prostaglandin E receptor subtype EP(2). Proc Natl Acad Sci USA 96: 10501–10506
23. Matzuk MM, Finegold MJ, Su J-GJ, Hsueh AJW, Bradley A 1992 α-Inhibin is a tumor-suppressor gene with gonadal specificity in mice. Nature 360:313–319
24. Couse JF, Hewitt SC, Bunch DO, Sar M, Walker VR, Davis BJ, Korach KS 1999 Postnatal sex reversal of the ovaries in mice lacking estrogen receptors α and β. Science 286:2328–2331
25. Eppig JJ, Chesnel F, Hirao Y, O'Brien MJ, Pendola FL, Watanabe S, Wigglesworth K 1997 Oocyte control of granulosa cell development: how and why. Hum Reprod 12:127–132
26. Brown CW, Houston-Hawkins DE, Woodruff TK, Matzuk MM 2000 Insertion of inhbb into the inhba locus rescues the inhba-null phenotype and reveals new activin functions. Nat Genet 25:453–457
27. Otsuka F, Yao Z, Lee T, Yamamoto S, Erickson GF, Shimasaki S 2000 Bone morphogenetic protein-15. Identification of target cells and biological functions. J Biol Chem 275:39523–39528
28. Bradley A 1987 Production and analysis of chimaeric mice. In: Robinson EJ (ed) Teratocarcinomas and Embryonic Stem Cells: A Practical Approach. IRL, Oxford. U.K., pp 113–151
29. Ramirez-Solis R, Rivera-Perez J, Wallace JD, Wims M, Zheng H, Bradley A 1992 Genomic DNA microextraction: a method to screen numerous samples. Anal Biochem 201:331–335
30. Wood DM, Dunbar BS 1981 Direct detection of two cross-reactive antigens between porcine and rabbit zonae pellucidae by radioimmunoassay and immunoelectrophoresis. J Exp Zool 217:423–433
31. Wood DM, Liu C, Dunbar BS 1981 Effect of alloimmunization and heteroimmunization with zonae pellucidae on fertility in rabbits. Biol Reprod 25:439–450
32. Prasad SV, Mujtaba S, Lee VH, Dunbar BS 1995 Immunogenicity enhancement of recombinant rabbit 55-kilodalton zona pellucida protein expressed using the baculovirus expression system. Biol Reprod 52:1167–1178
33. Prasad SV, Wilkins B, Skinner SM, Dunbar BS 1996 Evaluating zona pellucida structure and function using antibodies to rabbit 55 kDa ZP protein expressed in baculovirus expression system. Mol Reprod Dev 43: 519–529
34. Drell DW, Dunbar BS 1984 Monoclonal antibodies to rabbit and pig zonae pellucidae distinguish species-specific and shared antigenic determinants. Biol Reprod 30:445–457
35. Drell DW, Wood DM, Bundman D, Dunbar BS 1984 Immunological comparison of antibodies to porcine zonae pellucidae in rats and rabbits. Biol Reprod 30:435–444
36. Israel DI, Nove J, Kerns KM, Kaufman RJ, Rosen V, Cox KA, Wozney JM 1996 Heterodimeric bone morphogenetic proteins show enhanced activity in vitro and in vivo. Growth Factors 13:291–300
37. Aono A, Hazama M, Notoya K, Taketomi S, Yamasaki H, Tsukuda R, Sasaki S, Fujisawa Y 1995 Potent ectopic bone-inducing activity of bone morphogenetic protein-4/7 heterodimer. Biochem Biophys Res Commun 210: 670–677
38. Kusumoto K, Bessho K, Fujimura K, Akioka J, Ogawa Y, Iizuka T 1997 Comparison of ectopic osteoinduction in vivo by recombinant human BMP-2 and recombinant *Xenopus* BMP-4/7 heterodimer. Biochem Biophys Res Commun 239:575–579
39. Kumar TR, Wiseman AL, Kala G, Kala SV, Matzuk MM, Lieberman MW 2000 Reproductive defects in γ-glutamyl transpeptidase-deficient mice. Endocrinology 141: 4270–4277
40. Nishimori K, Young LJ, Guo Q, Wang Z, Insel TR, Matzuk MM 1996 Oxytocin is required for nursing but is not essential for parturition or reproductive behavior. Proc Natl Acad Sci USA 93:11699–11704